# The Initial Sintering of Alkaline Earth Oxides in Water Vapor and Hydrogen Gas

Tomoyasu Ito,* Masato Fujita, Masahiro Watanabe, and Taneki Tokuda
*Department of Chemistry, Faculty of Science, Tokyo Metropolitan University, Setagaya-ku, Tokyo 158*
(Received October 15, 1980)

The initial sintering (crystallite growth and surface-area diminution) of freely dispersed powders was studied. For MgO in $H_2O$ vapor, the sintering rate at 1073 K was directly proportional to the water-vapor pressure, $P_{H_2O}$, in the range of 27—2700 Pa, and the apparent activation energy, $E$, for the sintering was 137 kJ mol$^{-1}$. These facts lead to the conclusion that, in this system, the surface migration of $O^{2-}$ caused by the repetition of the adsorption-desorption cycle of the $H_2O$ molecule is rate-determining step for the sintering. For CaO in $H_2O$ vapor, the rate-determining step appears to be migration on and/or near the surface of a cation vacancy produced by the $H_2O$ adsorption, judging upon the facts that the sintering rate at 873 K was proportional to $P_{H_2O}^{0.34}$ in the range of 11—1600 Pa and that $E$ was 79.4 kJ mol$^{-1}$. For MgO in $H_2$ gas, the sintering rate at 1123 K was approximately proportional to the hydrogen pressure in the range of 3.3—66.5 kPa and $E$ was 310 kJ mol$^{-1}$, indicating that the sintering in $H_2$ was caused by $H_2O$ vapor formed upon the desorption of the surface hydroxyl groups which had been produced by a heterolytic dissociative adsorption of $H_2$.

Imperfections on the surface of polycrystalline oxide powders are known to have some remarkable effects on their adsorption behavior and catalytic nature. The properties and degrees of imperfections are controlled by the calcination conditions of the oxides. One of the most significant conditions is the atmosphere. Previously we have studied the initial sintering in 2.7 kPa water vapor of MgO powders originating from magnesium oxalate and reported a marked acceleration effect of $H_2O$ vapor.[1] A similar enhanced sintering for MgO in $H_2O$ vapor has been reported by several workers: (1) Anderson *et al.*[2] studied initial sintering at a relatively high temperature (1323 K) and suggested an adsorption-desorption cycle mechanism, but they did no kinetic analysis of their sintering data; (2) Razouk *et al.*[3] reported mainly changes in the micropore structure of MgO powders with sintering, and (3) Aihara *et al.*[4] studied changes in the crystallite size of MgO powders with sintering in 100-kPa $H_2O$ vapor and proposed an enhanced surface-diffusion mechanism. However, none of these studies has given clear evidence for the proposed mechanisms. A systematic investigation of initial sintering under strictly controlled experimental conditions seems to be necessary in order to clarify its mechanism.

In this paper, the initial sintering (which means the surface-area diminution and/or crystallite growth in the present study) of freely dispersed MgO powders was studied under various $H_2O$ pressures, and the mechanism of enhanced sintering was clarified by a kinetic analysis of the data on the pressure dependence of the sintering rate. A similar sintering study for CaO was carried out and compared with the case for MgO. Since a hydrogen molecule may be expected to produce a water molecule upon adsorption on the oxide surface at high temperatures, the sintering of MgO was also studied in a hydrogen atmosphere.

## Experimental

The processes for the sintering measurements were: (1) powders of 0.1-g magnesium oxalate dihydrate (0.33-g calcium hydroxide for CaO) in a Pt crucible mounted in a silica vessel were decomposed at 723 K (523 K for CaO) for 16 h under evacuation; then the resulting oxide was slowly heated to 1073 or 1123 K (873 K for CaO) and maintained at this temperature for 16 h under evacuation (this corresponds to sintering time= 0); (2) after cooling, the specific surface area was measured *in situ*; (3) after the sample had again been heated rapidly to the sintering temperature, $H_2O$ vapor or $H_2$ gas was admitted into the sintering vessel and the sintering was carried out in a closed system for a prescribed duration; (4) then Processes (2) and (3) were repeated, and the surface-area-diminution curves were obtained, and (5) finally, the crystallite size of sintered powders was measured by means of an X-ray diffractometer. For MgO in $H_2O$ vapor, an alternative method was used, a batch process consisting of the measurements of the surface area and crystallite size for each sintering run.

The hydrogen (Takachiho Chemicals, purity of 99.99% or more) was predried through a trap at 77 K. The specific surface area was measured by the BET method of oxygen adsorption at 77 K. For several samples, the distribution curve of the micropores smaller than 30 nm in diameter was obtained by the Cranston and Inkley method.[5] For the determination of the crystallite size, the (420) and (220) diffraction lines were used for MgO and CaO respectively. The crystallite size obtained by this method was somewhat larger ($<$10%) than that obtained by means of an electron micrograph.[1] For some samples, a volumetric adsorption amount of $H_2$ at the temperature used in the sintering was measured using a Pirani gauge. The equilibrium pressures in the adsorption study were around 10 Pa, much lower than that in the sintering study. Because a large part of the adsorption was completed within 5 min, this 5-min value is assumed to be an equilibrium-adsorption amount.

The magnesium oxalate dihydrate was prepared by two methods. The first batch (designated by MO-6) was prepared by a reaction of magnesium nitrate with ammonium oxalate, and the second batch (designated by MO-9), by a reaction of magnesium sulfate with ammonium oxalate. The magnesium oxalate dihydrate used was MO-6 unless otherwise stated in the text. The calcium hydroxide was prepared by burning calcium oxalate in air and by subsequent hydration with water free from carbon dioxide. The impurities, as determined by an atomic-absorption spectrometer, were as follows (weight ppm): MO-6: Mn=1.3, Fe$<$6.6; MO-9: Mn=4.6, Fe$<$8.6; $Ca(OH)_2$: Na=9.3, K$<$10, Mg=54. The emission spectra showed Ca in a concentration of 4—180 ppm in MO-6.

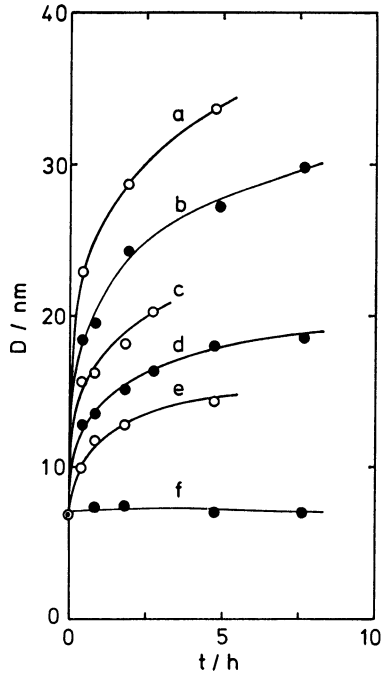


Fig. 1. Crystallite growth of MgO powders sintered at 1073 K in water vapor.
Pressure of water vapor/Pa: 2700 (a), 610 (b), 130 (c), 53 (d), 27 (e), and $<10^{-3}$ (*in vacuo*) (f).

## Results

*MgO in $H_2O$ Vapor.* The crystallite growth curves at 1073 K are shown in Fig. 1. The magnesium oxide powders before sintering had a crystallite size of about 7 nm. No appreciable growth occurred under evacuation ($<10^{-3}$ Pa), but water vapor exhibited remarkable positive effects for the growth rate. It has been established[1,4] that a crystallite growth rate is empirically expressed by:

$$\frac{dD}{dt} = \frac{k'_D}{D^{n'}}, \tag{1}$$

or by its integrated form:

$$D^n - D_0^n = k_D t, \tag{2}$$

where $D$ is the crystallite size ($D_0$ is $D$ at $t=0$), $t$ is the sintering time, $n$ ($=n'+1$) is a constant determined experimentally, and $k_D$ [$=k_D'(n'+1)$] is the rate constant

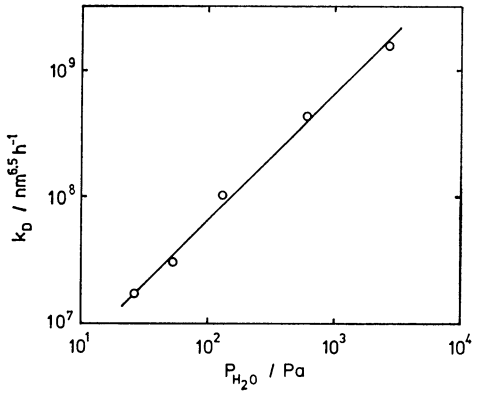


Fig. 2. Water vapor pressure dependence of crystallite growth rate constant at 1073 K for MgO powders.

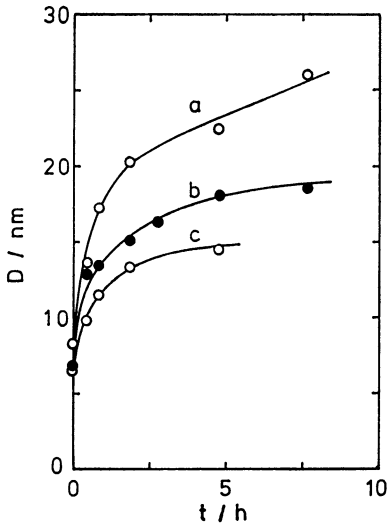


Fig. 3. Crystallite growth of MgO powders sintered in water vapor of 53 Pa.
Sintering temperature/K: 1173 (a), 1073 (b), and 973 (c).

for crystallite growth. The curves in Fig. 1 were well fitted to Eq. 2 if an appropriate value of $n$ was given. Therefore, the rate constants calculated by Eq. 2 were used for a quantitative comparison of the sintering rate, although this equation has no important physical meaning. In Fig. 2 the pressure dependence of $k_D$ is shown ($n=6.5$); the resultant straight line with a slope of 1.0 means that $k_D$ is directly proportional to the water-vapor pressure, $P_{H_2O}$. Crystallite growth curves at various temperatures are shown in Fig. 3. The rate constants calculated by Eq. 2 gave an apparent activation energy for the crystallite growth of 137 kJ mol$^{-1}$ which agrees with that obtained by Aihara *et al.*[4]

If the secondary agglomeration between crystallites is ignored, an ideal specific surface area, $S_x$, as calculated from the observed crystallite size, is expressed by:

$$S_x = \frac{6}{\rho} \cdot \frac{1}{D}, \tag{3}$$

where $\rho$ is the density of the sample. For the MgO powders sintered in water vapor, the observed specific surface area, $S$, was roughly proportional to the inverse of the crystallite size observed, and the degree of the secondary agglomeration scarcely changed at all during the sintering ($S/S_x=0.55$—$0.65$). These facts indicate that the surface-area reduction was a direct consequence of the crystallite growth. Therefore, an equation similar to Eq. 2 is also applicable to the surface-area diminution:

$$S^m - S_0^m = k_s t, \tag{4}$$

where $m$ ($\approx -n$) is a constant determined experimentally, $S_0$ is $S$ at $t=0$, and $k_s$ is the rate constant for the surface-area decrease. The temperature dependence of $k_s$ gave an apparent activation energy of 131 kJ mol$^{-1}$, which is in good agreement with that for $k_D$.

The micropore distributions are shown in Fig. 4 for several samples sintered at 1073 K for 2 h. No samples had micropores below 1.5 nm in diameter. As the sintering proceeded, micropores with smaller diameters disappeared preferentially and larger ones grew. The

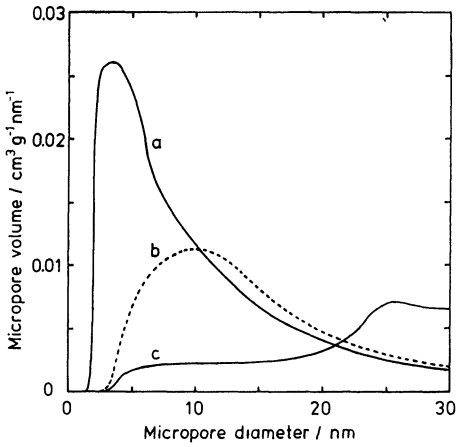


Fig. 4. Micropore distribution of MgO powders sintered at 1073 K for 2 h in water vapor.
Pressure of water vapor/Pa: $<10^{-3}$ (*in vacuo*) (a), 27 (b), and 2700 (c).

Table 1. Micropores of MgO powders sintered at 1073 K for 2 h in water vapor

| $P_{H_2O}$ / Pa | Total volume of micropore / $cm^3\ g^{-1}$ | Diameter of micropore at maximum distribution/nm | Specific surface area / $m^2\ g^{-1}$ |
|---|---|---|---|
| $<10^{-3}$ (*in vacuo*) | 0.265 | 3.5 | 165.2 |
| 27 | 0.178 | 10 | 62.3 |
| 2700 | 0.090 | 25 | 26.2 |

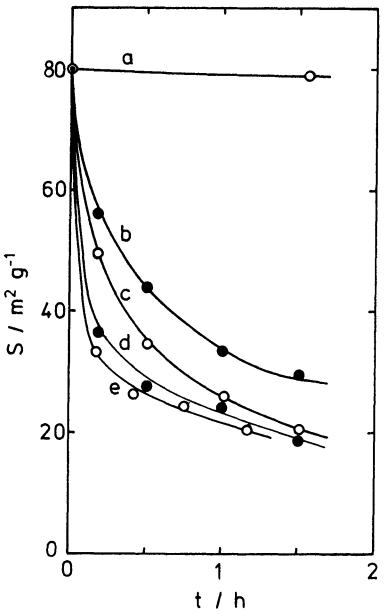


Fig. 5. Surface area decrease of CaO powders sintered at 873 K in water vapor.
Pressure of water vapor/Pa: $<10^{-3}$ (*in vacuo*) (a), 11 (b), 110 (c), 610 (d), and 1600 (e).

resultant micropore volumes are summarized in Table 1.

*CaO in $H_2O$ Vapor.* The surface area decreases upon the sintering in various $P_{H_2O}$ values at 873 K are shown in Fig. 5. Calcium oxide powders, before sintering, had a specific surface area of about 80 $m^2\ g^{-1}$; this area decreased little during sintering under evacuation. On the other hand, $H_2O$ vapor accelerated the sintering for CaO, which was more remarkable than for MgO. Although there is some scatter, a value of $m=-3.2$ nearly satisfied Eq. 4 for this sintering system. It can be found from Fig. 6 that $k_s$ is proportional to $P_{H_2O}^{0.34}$ in the range of 11—1600 Pa. Figure 7 illustrates the reduction of $S$ at various sintering temperatures for $P_{H_2O}=610$ Pa. The apparent activation energy as estimated by Eq. 4 was 79.4 kJ $mol^{-1}$, which is smaller than that for MgO in $H_2O$ vapor. The values of $S/S_x$ were in the range of 0.5—0.6 for all the samples, and no important changes in the secondary agglomeration were observed during the sintering process. The micropore distributions for three samples sintered to different extents are shown in Fig. 8. No samples had micropores below 2.5 nm in diameter. As the sintering proceeded, micropores with smaller diameters rapidly disappeared,

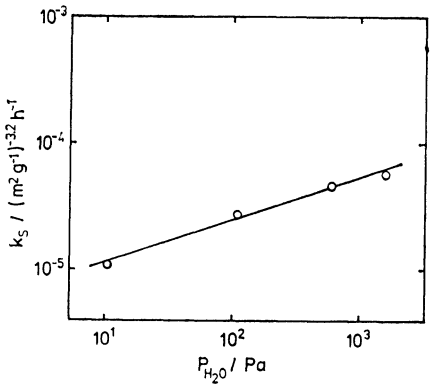


Fig. 6. Water vapor pressure dependence of sintering rate constant at 873 K for the surface area diminution of CaO powders.

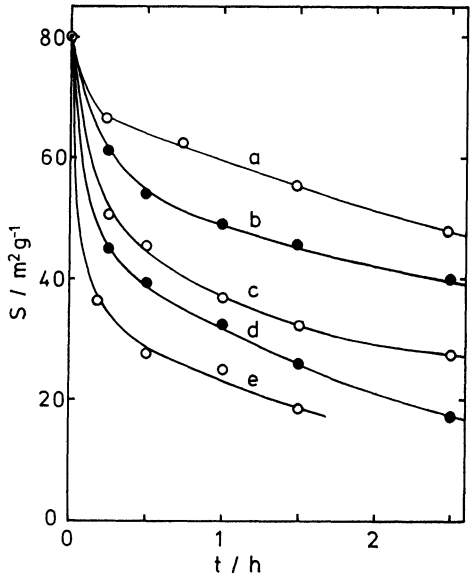


Fig. 7. Surface area diminution of CaO powders sintered in water vapor of 610 Pa.
Sintering temperature/K: 673 (a), 723 (b), 773 (c), 823 (d), and 873 (e).

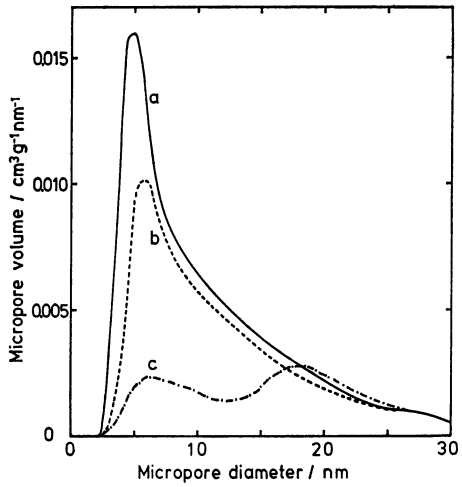


Fig. 8. Micropore distribution of CaO powders sintered in water vapor.
Sintering conditions (temperature/K—pressure/Pa—time/h): 873—$<10^{-3}$ (*in vacuo*)—0 (a), 673—610—2.5 (b), and 873—1600—1.2 (c).

TABLE 2. MICROPORES OF CaO POWDERS SINTERED IN WATER VAPOR

| Sintering condition[a)] | Total volume of micropore / $cm^3\ g^{-1}$ | Diameter of micropore at maximum distribution/nm | Specific surface area / $m^2\ g^{-1}$ |
|---|---|---|---|
| 873—$<10^{-3}$—0 | 0.131 | 5 | 80.0 |
| 673—610—2.5 | 0.097 | 6 | 48.1 |
| 873—1600—1.2 | 0.052 | 6, 18 | 18.0 |

a) Temperature/K—$P_{H_2O}$/Pa—time/h.

as in the case of MgO. The micropore volumes are summarized in Table 2.

*MgO in $H_2$ Gas.* Figure 9 shows the change of $S$ in an $H_2$ atmosphere at 1123 K. Hydrogen evidently increased the sintering rate, but its efficiency was far less than that of $H_2O$. A value of $-6.0$ for $m$ in Eq. 4 gave the best fit for all the observed data. The pressure dependence of $k_s$ is shown in Fig. 10; the slope of the straight line obtained was 0.9. The sintering-rate constants observed at three temperatures (1023, 1073, and 1123 K) in 33.3 kPa $H_2$ gave an apparent activation energy of 310 kJ $mol^{-1}$, more than twice that in an $H_2O$ atmosphere.

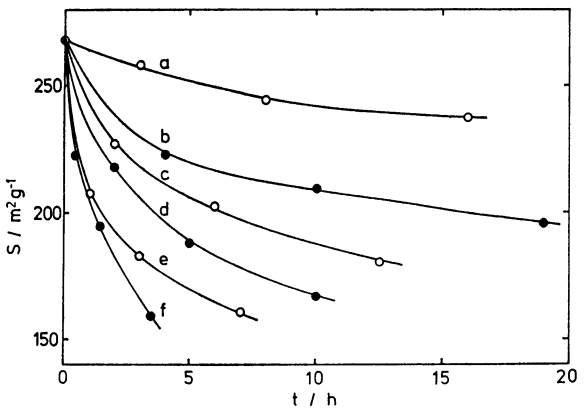


Fig. 9. Surface area decrease of MgO powders sintered at 1123 K in hydrogen gas.
Hydrogen pressure/kPa: $<10^{-3}$ (*in vacuo*) (a), 3.3 (b), 5.3 (c), 13.3 (d), 33.3 (e), and 66.5 (f).

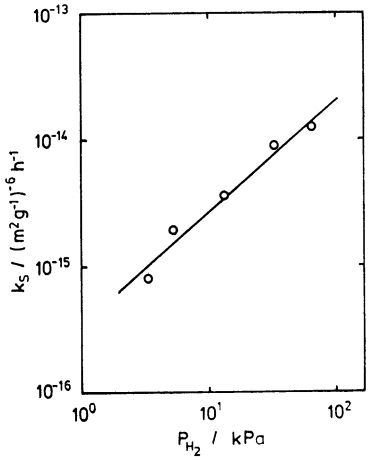


Fig. 10. Hydrogen pressure dependence of sintering rate constant at 1123 K for the surface area diminution of MgO powders.

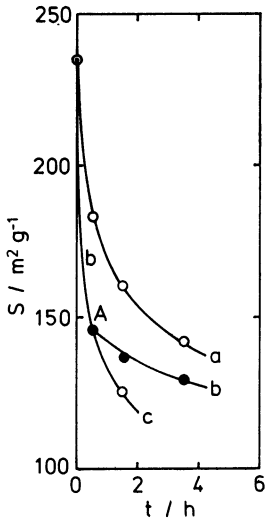


Fig. 11. Effect of Pre-oxidation on surface area decrease of MgO powders (MO-9 origin) sintered at 1123 K in hydrogen gas of 20 kPa.
Pretreatment: (a) no oxidation (normal sintering), (b) 1 h evacuation after oxidation by 13.3 kPa oxygen gas for 1 h at 1123 K, and (c) 1 h evacuation after re-oxidation at point A in curve (b).

If the sample was oxidized by $O_2$ before sintering, an unusual sintering behavior was observed. Figure 11 shows the sintering of MgO (MO-9 origin) at 1123 K in a 20 kPa $H_2$ atmosphere. Curve (a) illustrates a normal sintering (namely, without $O_2$ pretreatment), while Curve (b) shows the sintering of the sample pretreated by 13.3 kPa $O_2$ at 1123 K for 1 h and a subsequent outgassing for 1 h. In this case, the rate constant in the first run (before Point A) was about 4 times larger than that after the second, the latter being of a magnitude comparable to that of Curve (a). If the

sample was reoxidized at Point A, a faster rate was also observed in the second run, as is shown by Curve (c). The amounts of $H_2$ adsorbed at 1123 K on MgO (MO-9 origin) with a specific surface area of 210 $m^2\,g^{-1}$ were 14.1, 1.2, and $13.1\times10^{18}$ molecule $g^{-1}$ after oxidation for 1 h followed by evacuation for 1 h, evacuation for 1 h after the first $H_2$ adsorption, and reoxidation after the second $H_2$ adsorption respectively. It is, therefore, understandable that the sintering rate depends on the adsorption amount. Similar behavior was also observed for MgO prepared from MO-6, though the sintering rates were different between MO-9 and MO-6.

## Discussion

*Sintering Mechanism in $H_2O$ Vapor.* Because no appreciable sintering occurred in a vacuum, it can easily be understood that the enhanced sintering in $H_2O$ vapor was caused by the adsorption effect. Unfortunately, we have little information on the chemisorption of $H_2O$ on alkaline earth oxides at high temperatures. Previously we reported an IR study of $H_2O$ adsorbed on MgO, revealing that only hydroxyl groups (two types, namely, free and hydrogen-bonded $OH^-$) were present at 773 K, while physisorbed molecules coexisted below 673 K.[6] This suggests that the species adsorbed on MgO in the present study are also hydroxyl groups. The adsorption amounts (in terms of the apparent surface coverage) thus far reported are 0.15[7] (in 0.8 kPa $H_2O$ vapor at 923 K) and $<0.005$[2] (in 0.6 kPa at 1273 K). The expected coverages on MgO in the present case, typically carried out at 1073 K, may, therefore, be of the order of 0.01—0.02. For CaO, the adsorbed species may also be hydroxyl groups, but the adsorption amounts appear to be considerably larger than for MgO because of its stronger interaction with a water molecule and because of the lower temperature used for the sintering.

Possible sintering mechanisms include: (1) a diffusion mechanism (surface, grain-boundary, and bulk); (2) a viscous-flow mechanism; (3) an evaporation-condensation mechanism, and (4) an adsorption-induced space-charge mechanism. Furthermore, we must consider (5) the adsorption-desorption-cycle mechanism (anion-exchange mechanism) proposed by Anderson *et al.*,[2] because the free surface of the powders used is relatively large. This mechanism gives a mode of transport for a surface $O^{2-}$ ion through the process by which, upon the desorption of an $H_2O$ molecule, an oxygen ion from the surface may be removed in the desorbing $H_2O$ molecule, leaving the $O^{2-}$ of the original $H_2O$ in an adjacent position on the surface. Of the five possibilities mentioned above, Mechanisms (3) and (4) can be disregarded because of the too low vapor pressure and because of no generation of a new space charge respectively. Mechanisms (1) and (2) both depend on an equilibrium amount of $H_2O$ adsorbed on the oxide under the present experimental conditions [in Mechanism (1), the rate is proportional to the adsorbed amounts to the first power, and in (2), to the second power], and Mechanism (5) depends on the frequency of the adsorption-desorption cycle of $H_2O$ molecules under a dynamic adsorption equilibrium. Therefore, we will consider these two cases in more detail.

In the first case, a sintering rate constant, $k$, is proportional to the equilibrium adsorption amount, $v$, to the first or the second power. Because an $H_2O$ molecule can be assumed to be adsorbed on a cation-anion pair site (designated by S) on the surface and results in the formation of $OH^-$, the adsorption equilibrium near the surface is expressed by:[8]

$$S + H_2O \overset{K_1}{\rightleftharpoons} 2\,OH^- + V_M, \tag{5}$$

where $V_M$ is the cation vacancy and $K_1$ is an equilibrium constant. From Eq. 5,

$$v \equiv [V_M] = \frac{1}{2}[OH^-] = \left\{\frac{K_1}{4}\cdot[S]\cdot P_{H_2O}\right\}^{1/3}. \tag{6}$$

On the other hand, $v$ can also be expressed by:

$$v = [S]_0 - [S] = [S]_0\theta, \tag{7}$$

where $\theta$ is the (apparent) surface coverage and where the subscript 0 refers to a state before the adsorption. By substituting Eq. 7 into Eq. 6 and by differentiating its logarithmic form, we obtain:

$$\frac{d\ln v}{d\ln P_{H_2O}} = \frac{1}{3}\cdot\frac{3-3\theta}{3-2\theta}. \tag{8}$$

If $k$ is proportional to $v$ [Mechanism (1)], then

$$l \equiv \frac{d\ln k}{d\ln P_{H_2O}} = \frac{1}{3}\cdot\frac{3-3\theta}{3-2\theta}, \tag{9}$$

that is, $k$ is proportional to $P^l_{H_2O}$ at a coverage of $\theta$. If $k$ is proportional to $v^2$ [Mechanism (2)], then

$$l = \frac{2}{3}\cdot\frac{3-3\theta}{3-2\theta}. \tag{10}$$

In the second case, $k$ is proportional to the frequency, $R$, of the adsorption-desorption cycle. When the absolute-rate theory is applied, $R$ depends on where the rate-determining step is. If, for example, an adsorption process is rate-determining, the following two reaction schemes are possible:

$$\left.\begin{aligned} &H_2O + S \overset{K_2}{\rightleftharpoons} I \\ &I \overset{k_2}{\longrightarrow} 2\,OH^- + V_M, \end{aligned}\right\} \tag{11}$$

and

$$\left.\begin{aligned} &H_2O + S \overset{K_3}{\rightleftharpoons} 2\,I \\ &I \overset{k_3}{\longrightarrow} OH^- + \frac{1}{2}V_M, \end{aligned}\right\} \tag{12}$$

where I designates an activated complex and where $k_i$ and $K_i$ are the rate constant and the equilibrium constant respectively. The former corresponds to an undissociated activated complex, and $R$ is expressed by:

$$R = k_2\cdot[I] = k_2\cdot K_2\cdot[S]\cdot P_{H_2O}, \tag{13}$$

while the latter corresponds to a dissociated activated complex:

$$R = 2k_3\cdot[I] = 2\,k_3\cdot K_3^{1/2}\cdot[S]^{1/2}\cdot P_{H_2O}^{1/2}. \tag{14}$$

A further examination of other cases (*e. g.*, the presence of a pre-adsorption equilibrium, and the desorption process being a rate-determining step) revealed that either Eq. 13 or 14 is applicable to every case (except for

the constants in them). Therefore, the frequency of the adsorption-desorption cycle is expressed by either:

$$\left.\begin{aligned} R &= c \cdot [S] \cdot P_{H_2O} \\ \text{or} \\ R &= c \cdot [S]^{1/2} \cdot P_{H_2O}^{1/2}, \end{aligned}\right\} \quad (15)$$

where $c$ is a constant. In a manner similar to the first case, we can obtain final expressions corresponding to the two cases in Eq. 15:

$$l = \frac{3-3\theta}{3-2\theta} \quad (16)$$

$$l = \frac{1}{2} \cdot \frac{3-3\theta}{3-2\theta}. \quad (17)$$

Figure 12 shows the values of $l$ in Eqs. 9, 10, 16, and 17. Now we can compare the observed data with the calculated values.

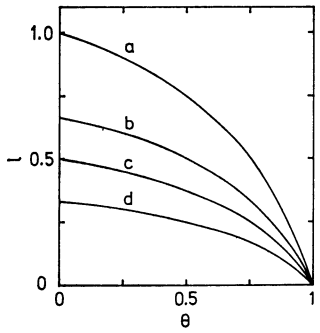


Fig. 12. Dependence of sintering rate constant on apparent surface coverage.
(a): Eq. 16 [mechanism (5)], (b): Eq. 10 [mechanism (2)], (c): Eq. 17 [mechanism (5)], and (d): Eq. 9 [mechanism (1)].

*MgO in $H_2O$ Vapor.* The experimental facts were that $l$ equals 1 in the $P_{H_2O}$ range of 27—2700 Pa at 1073 K and that the apparent activation energy of the crystallite growth is 137 kJ mol$^{-1}$. It may be found from Fig. 12 that $l$ becomes 1 only when $\theta \approx 0$ in Eq. 16. As has been described previously, $\theta \approx 0$ (say, $\theta < 0.1$) was fulfilled in the present case. It may be concluded, therefore, that, for MgO in $H_2O$ vapor, an anion-exchange mechanism is operative and that surface $O^{2-}$ ions move on the surface by repeating the adsorption-desorption cycle of $H_2O$ molecules. The measurement of the isotopic-exchange-reaction rate of oxygen atoms between $H_2O$ and surface $O^{2-}$ at high temperatures can afford useful information, but we could not succeed in its measurement because of the too rapid exchange rate and because of the peculiar nature of $H_2O$ vapor. We can see, however, on the basis of simple gas kinetics, that each adsorbing center of the oxide surface is subjected to a collision with an $H_2O$ molecule $\approx 10^5$ times per second under typical sintering conditions and that the time of residence of an $H_2O$ molecule at the surface is sufficient for the molecule to interact with the surface.[2] On the other hand, the cations may easily move on or near the surface by the diffusion of the $V_M$ formed.

There are no micropores with diameters $<1.5$ nm in any sample (Fig. 4). Therefore, the sintering by the anion-exchange mechanism is thought to proceed mainly, not through condensation between two surface $OH^-$ ions of adjacent crystallites in a micropore, thus forming an oxygen bridge between the crystallites and to form a closed micropore, but through condensation between two adjacent $OH^-$ ions on a crystallite, thus leading to an enhanced surface mobility which causes the disappearance of smaller crystallites and the growth of larger ones. This picture is in accord with the finding that $S/S_x$ did not change appreciably during the sintering.

Eastman *et al.*[8] and Mackenzie *et al.*[9] suggested an association of two $OH^-$ and $V_M$ in Eq. 5 and the formation of a complex such as $2OH^- \cdot V_M$. However, this seems not to be valid in the present case considering the two facts that: (1) a completely linear relationship between $k$ and $P_{H_2O}$ holds, even for $P_{H_2O} < 100$ Pa (Fig. 2), and (2) for the CaO sintering, $k$ is proportional to $P_{H_2O}^{0.34}$, suggesting non-association between adsorbed species, even though much more $OH^-$ and $V_M$ are present compared to the case of MgO.

*CaO in $H_2O$ Vapor.* It was found experimentally that $l$ equals 0.34 in the $P_{H_2O}$ range of 11—1600 Pa at 873 K and that the apparent activation energy for $k$ is 79.4 kJ mol$^{-1}$. From Fig. 12, $l=0.34$ is possible in the four cases; namely, $\theta \approx 0$ in Eq. 9, $\theta \approx 0.75$ in Eq. 10, $\theta \approx 0.85$ in Eq. 16, and $\theta \approx 0.6$ in Eq. 17. However, it seems to be impossible, unless $\theta \approx 0$ or 1, that a constant value of $l$ is maintained during about a 150-fold change in $P_{H_2O}$ (11—1600 Pa). Thus, Eqs. 10, 16, and 17 can be excluded, and only the case of $\theta \approx 0$ in Eq. 9 is applicable; that is, the sintering proceeds through a diffusion mechanism ($\theta \approx 0$ suggests that the adsorbed species are present not only on the surface, but also beneath the surface). We must then determine which of the adsorbed species, $V_M$ or $OH^-$, is concerned with the rate-determining step. It may be possible for an anion on the surface to migrate by means of an anion-exchange mechanism, by analogy with MgO, and a cation in CaO is less movable than one in MgO because of the larger cation size and heavier atomic mass. Therefore, we suggest that $V_M$ is the rate-determining species and that it moves on and/or near the surface layer.

Let us now look at the apparent activation energy of the sintering rate. If the above mechanism is assumed to be valid, $k$ is expressed by:

$$k = k_d \cdot [V_M], \quad (18)$$

where $k_d$ is a diffusion coefficient of $V_M$. By substituting Eq. 6 into Eq. 18, assuming $P_{H_2O}$=constant and [S]= constant (because of $\theta \approx 0$), and differentiating by temperature, $T$, the logarithmic form of a resultant equation, we obtain:

$$\frac{d \ln k}{dT} = \frac{d \ln k_d}{dT} + \frac{1}{3} \cdot \frac{d \ln K_1}{dT}. \quad (19)$$

Using an Arrhenius equation and a van't Hoff equation, we then obtain:

$$E = E_d - \frac{Q}{3}, \quad (20)$$

where $E$ is the apparent activation energy for the sintering rate, $E_d$ is the activation energy for the diffusion of $V_M$, and $Q$ is the heat of the adsorption of Eq. 5. Unfortunately, there are no appropriate values for $E_d$ and $Q$. However, if we are allowed to use, as $E_d$, the value of 118 kJ mol$^{-1}$ of the activation energy for $Ca^{2+}$ bulk-diffusion at 1273—1673 K[10] and, as $Q$, the 96 kJ mol$^{-1}$ of the heat of the dissociation reaction,[11] $Ca(OH)_2 \rightleftharpoons CaO + H_2O$, then we obtain $E$=86 kJ mol$^{-1}$. On and/or near the surface, $E_d$ and $Q$ are probably smaller than those in bulk, but the resultant $E$ as a difference between them may be expected to be not far from the observed value of 79.4 kJ mol$^{-1}$. This suggests the validity of the concepts that, for CaO in $H_2O$ vapor, a diffusion of $V_M$ on and/or near the surface is rate-determining and that the anion easily migrates on the surface by means of an anion-exchange mechanism.

*Sintering Mechanism in $H_2$.* It has been established that $H_2$ is adsorbed on MgO at high temperatures, and that the higher the temperature, the more the adsorption amount.[12-14] The adsorbed species have been identified as hydroxyl groups by Lisachenko *et al.*[12] Therefore, the desorption from the heated sample under a dynamic adsorption equilibrium can produce an $H_2O$ molecule from two adsorbed $OH^-$.[12,14] If the resultant pressure of $H_2O$ vapor present in the 10 kPa $H_2$ atmosphere reaches only 0.1 Pa, it is possible to explain the observed sintering shown in Fig. 9. Unfortunately, we failed to confirm, by the use of a mass-spectrometer, the presence of water vapor in a large excess of $H_2$ or $D_2$ gas after the sintering because of its too small quantity, the presence of background peaks, the easy adsorption of water vapor onto the wall, *etc.* However, as has previously been described, the amount of $H_2$ adsorbed on MgO at 1123 K was $1.2 \times 10^{18}$ molecule g$^{-1}$ even for the second run, which corresponds to an $H_2O$ partial pressure of 100 Pa if all the adsorbed species are assumed to be desorbed as $H_2O$ molecules. Therefore, it is very possible that the actual partial pressure of $H_2O$ in $H_2$ reaches 0.1 Pa. Below we will discuss the sintering mechanism based upon the view that the initial sintering in $H_2$ is caused by the $H_2O$ molecules formed.

It was found experimentally for MgO in $H_2$ gas that $l$ equals 0.9 in the $H_2$ pressure range of 3.3—66.5 kPa at 1123 K and that the apparent activation energy for the sintering is quite large, 310 kJ mol$^{-1}$. The formation of hydroxyl groups upon the $H_2$ adsorption may be possible through: (1) the reduction of trace amounts ($<$100 ppm) of the transition elements present; (2) a reaction with an $O^-$ ion[15] present on the activated surface; (3) the reduction of $Mg^{2+}$, and (4) the heterolytic dissociation of $H_2$ into $H^+$ and $H^-$. Mechanisms (1)—(3) are, however, unimportant in the present case because of the disagreements with the actual concentrations and/or with the actual pressure dependences. Therefore, we will consider Mechanism (4) in some detail. Unfortunately, the direct observation of a Mg–H (possibly $Mg^{2+}$–$H^-$) stretching frequency by means of the IR spectra is very difficult at the temperatures used in the sintering study. However, recently Coluccia *et al.*[16] reported on the IR spectra upon the $H_2$ adsorption at room temperature on MgO activated at high temperatures, and proved the formation of O–H and Mg–H bonds. According to our temperature-programed desorption study,[17] these adsorbed species remain on the surface up to around 700 K, even under a high vacuum. Thus, a similar adsorption scheme appears to be possible for the present sintering experiment. This adsorption equilibrium is expressed by:

$$\left.\begin{aligned} H_2 + O^{2-} &\overset{K_4}{\rightleftharpoons} OH^- + H^- + V_M \\ 2\,OH^- + V_M &\overset{K_5}{\rightleftharpoons} H_2O + O^{2-}. \end{aligned}\right\} \quad (21)$$

Therefore,

$$P_{H_2O} = K_4 \cdot K_5 \cdot \frac{[OH^-]}{[H^-]} \cdot P_{H_2}, \quad (22)$$

where $P_{H_2O}$ and $P_{H_2}$ are the partial pressures of $H_2O$ and $H_2$ respectively. Equation 22 shows that, unless the change in $P_{H_2}$ is large, $P_{H_2O}$ is approximately proportional to $P_{H_2}$. This agrees with the experimental facts, for the sintering rate in $H_2O$ vapor is simply proportional to $P_{H_2O}$, as has been mentioned previously. The activation energy of the sintering for this mechanism is expected to be larger than that in a pure $H_2O$ vapor by the heat of reaction necessary for Eq. 21. Though qualitative, this can explain the observed results (137 kJ mol$^{-1}$ for $H_2O$ and 310 kJ mol$^{-1}$ for $H_2$). It may be concluded, therefore, that the enhanced sintering in $H_2$ gas proceeds by means of an anion-exchange mechanism caused by $H_2O$ vapor which has been produced upon the heterolytic dissociative adsorption of $H_2$ on the surface at a high temperature (Eq. 21).

Prior to the sintering, the MgO sample was usually preevacuated at 1123 K for a long time without oxidation. On the other hand, the sample preoxidized at 1123 K exhibited a remarkable sintering upon the first $H_2$ admission (Fig. 11). This is explicable by considering that each adsorption equilibrium of the four possible mechanisms on $OH^-$ formation described above was shifted to the oxidation side and subsequent admission of $H_2$ produced more $H_2O$ vapor than usual.

Guilliatt *et al.*[18] carried out a crystallite-growth study of MgO in the $H_2$ atmosphere of, not a closed, but a flowing system, and found no substantial effectiveness of an $H_2$ gas for sintering. On the other hand, in the closed (static) system used in the present study, some remarkable effects were observed. One must pay much attention to these differences in the experimental conditions upon the measurements of various properties of solids, such as their sintering behavior and electric conductivity.

## References

1) T. Ito and T. Tokuda, *Nippon Kagaku Kaishi*, **1974**, 248.
2) P. J. Anderson and P. L. Morgan, *Trans. Faraday Soc.*, **60**, 930 (1964).
3) R. I. Razouk, R. Sh. Mikhail, and J. Ragai, *J. Appl. Chem. Biotechnol.*, **23**, 51 (1973).
4) K. Aihara and A. C. D. Chaklader, *Acta Metall.*, **23**, 855 (1975).
5) R. W. Cranston and F. A. Inkley, "Adv. in Catalysis," Academic Press, New York (1957), Vol. 9, p. 143.
6) T. Ito, K. Kanehori, and T. Tokuda, *Z. Phys. Chem., N. F.*, **103**, 203 (1976).

7) A. G. Oblad, S. W. Weller, and G. A. Mills, Proc. 2nd Int. Congr. Surface Activity, London (1957), Vol. 2, 309.
8) P. F. Eastman and I. B. Cutler, *J. Am. Ceram. Soc.*, **49**, 526 (1966).
9) K. J. D. Mackenzie and P. J. Melling, *Trans. J. Brit. Ceram. Soc.*, **73**, 23 (1974).
10) V. Kumer and Y. P. Gupta, *J. Phys. Chem. Solids*, **30**, 677 (1969).
11) J. A. C. Samms and B. E. Evans, *J. Appl. Chem.*, **18**, 5 (1968).
12) A. A. Lisachenko and V. N. Filimonov, *Dokl. Akad. Nauk SSSR*, **177**, 391 (1967); A. A. Lisachenko and F. I. Vilesov, *Kinet. Katal.*, **13**, 749 (1972).
13) D. Cordischi, R. L. Nelson, and A. J. Tench, *Trans. Faraday Soc.*, **65**, 2740 (1969).
14) K. V. Topchieva, A. Yu. Loginov, and T. M. Semenkina, *Vestn. Mosk. Univ., Khim.*, **16**, 276 (1975).
15) R. Martens, H. Gentsch, and F. Freund, *J. Catal.*, **44**, 366 (1976).
16) S. Coluccia and A. J. Tench, Preprints of 7th Int. Congr. Catalysis, Tokyo (1980), B35.
17) T. Ito, T. Sekino, N. Moriai, and T. Tokuda, *J. Chem. Soc., Faraday Trans. 1*, in press.
18) I. F. Guilliatt and N. H. Brett, *J. Chem. Soc., Faraday Trans. 1*, **68**, 429 (1972).